Modified High Level DC-DC Converter Based Online Transformerless Uninterruptible Power Supply (UPS)

[1]Shruthi S, [2]Neetha H M, [3]Kiran Kumar G R, [4]Kalpana S

[1,2,3,4]Assistant Professor
Department of Electricals & Electronics Engineering
PES Institute of Technology and Management, Shivamogga, Karnataka, India

Abstract: **To provide reliable and high quality power for critical loads in all grid conditions, Uninterruptible Power Supplies (UPS) are widely used. A non-isolated online uninterruptible power supply (UPS) system is proposed in this paper. This system consists of bridgeless PFC boost rectifier, battery charger/discharger, and an inverter. A new battery charger/discharger has been implemented which ensures the bidirectional flow of power between dc-link and battery bank, reducing the battery bank voltage to only 24V, and regulates the dc-link voltage during battery power mode. Operating batteries in parallel improves the battery performance and resolve the problems related to conventional battery banks that arrange batteries in series. The output voltage for both linear and non-linear loads regulating system is proposed which contains a new control method, integrating slide mode and proportional-resonant control, for inverter. The controller exhibits excellent performance during transients and step changes in load. Operating principle and experimental results of 1kVA prototype have been presented for validation of the proposed system.**

Index Terms: Uninterruptible power supply, Battery charger/discharger, Power factor correction, transformerless UPS;

I. INTRODUCTION

Uninterruptible power supplies (UPS) provide clean, conditioned, and reliable power to critical loads such as communication systems, network servers, medical equipment's etc. in all grid conditions [1, 2]. Typically the UPS provides unity power factor, high efficiency, high reliability, low cost, and low transients response time from grid mode to battery mode and vice versa [3, 4].

UPS systems can be categorized as online, offline, and line interactive UPS systems [5]. Online UPS systems are most popular and common configuration among them, as it provides isolation to load from the grid and has negligible switching time. Conventional online UPS system consists of rectifier for PFC, battery bank, and an inverter connected to the load [6]. Grid frequency transformers are normally employed to reduce the battery bank voltage and provide isolation from the transients and spikes generated inside the grid. Since the transformer is operating at line frequency, thus increasing the size and weight of the system substantially. Online UPS system with high frequency transformer isolation has been used to overcome the problem related to grid frequency transformer UPS system [7]. Although the size has been reduced, the efficiency of the system decreases due to high number of active switches in these topologies.

In order to overcome the problems related to aforementioned topologies, the transformerless UPS system has been introduced. Transformerless UPS systems have comparatively high efficiency, small weight and volume of the system. The only disadvantage in transformerless UPS system is their susceptibility towards the interference caused by the devices connected to the same grid. This makes the transformerless UPS more suitable for environments where the connected grid is less polluted [8].

Several transformerless topologies has been proposed in [9-12], focusing on efficiency improvement, volume and weight reduction, decreasing the number of switches, and capital cost of the system. But the size of the battery bank in all the proposed systems so far is enormously high. Generally, the batteries are connected in series to achieve high battery bank voltage. But series battery arrangement has major drawbacks and limitations in charging and discharging. Small imbalance in voltages occurs across the battery cells during charging and discharging since battery cells are not equal. Hence, these cannot provide the same performance during operation. Overcharging will cause severe overheating, low performance, and even destruction [13]. Similarly, deep discharge may cause the battery cell to be damaged permanently [14]. Due to this reason, small battery bank with batteries operating in parallel improves the performance of the battery bank significantly. The batteries operating in parallel have following advantages;

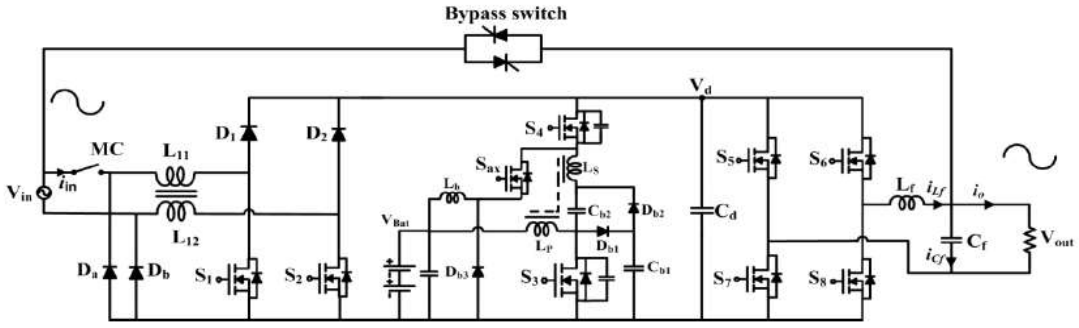

Figure. 1. Circuit diagram of the proposed UPS system

1. The number of batteries is not restricted to the dc-link voltage. The volume, weight and backup time of the battery bank should be designed according to specific application.
2. Cost reduction as no extra voltage balancing circuit is required.
3. Damaged batteries can be isolated or replaced from the battery bank, thus, leaving the sensitive system operation uninterrupted. This is prime function of UPS system.
4. Since discharging currents of the batteries can be profiled individually. Hence, the stored energy in the batteries can be utilized more efficiently.

A UPS topology is proposed in [5] which employs only three leg converter for both rectification and dc-ac conversion. But the battery bank of 360V is connected to the dc-link, which is enormously high and all the current drawn by the batteries is pulsating. This pulsating current affects the reliability of the battery bank. In [6], a transformerless UPS has been proposed with bidirectional battery charger and discharger connected to the battery bank. But still the battery bank is very high and is not suitable for low power applications. Non-isolated topology of UPS system has been proposed in [7]. It reduces the battery bank to nine batteries but it employs an auto-transformer to achieve high dc-link voltage that increases the size and weight of the system.

In this paper, a novel transformerless online UPS has been proposed as shown in Fig. 1. The proposed UPS employs a high gain bidirectional converter which operates between the dc-link voltage and battery bank. Using bidirectional charger/discharger, the battery bank is reduced to only 24V (single battery), thus, it eliminates the drawbacks related to large string of series connected batteries. The bridgeless boost rectifier provides the regulated dc-link voltage to feed inverter and maintains the power factor correction. A new controller combining slide mode and proportional-resonant (PR) control has been implemented for the inverter control which shows good performance with low total harmonics distortion (THD) and high stability for both non-linear and impulsive loads. The size and cost of the proposed system is comparatively very low as no bulky transformer has been used, with small battery bank and high efficiency. Hence, the proposed UPS system is excellent choice for low power application with low cost and weight of the system.

Experimental results based on 1kVA laboratory prototype have been presented to validate the performance of the system. The proposed UPS system shows excellent steady state and dynamic performance. The advantages of the proposed system are as follows. 1) New battery charger and discharger has been introduced which reduce the size of the battery bank significantly. 2) High input power factor. 3) New robust inverter control scheme for non-linear and impulse load. 4) High efficiency and low cost of the system.

II. PROPOSED SYSTEM TECHNIQUES

The schematic of the proposed single phase online UPS system is shown in Fig. 1. The proposed system consists of a bridgeless PFC boost rectifier, a bidirectional converter, and an H-bridge inverter. The boost rectifier provides the power factor correction and regulated dc-link voltage. The efficiency of the bridgeless rectifier is also high as compared to conventional rectifiers because it eliminates some devices from the power flow path and reduces the conduction losses considerably. Introducing a bidirectional converter for battery charging and discharging with high voltage gain reduces the size of battery bank significantly. The H-bridge inverter with new robust control scheme is proposed for regulating the non-linear load and provides fast transient response during change of modes.

A. Modes of operation

The operation of the UPS can be divided into two modes of operation. Grid mode and battery mode as shown in the Fig. 2.

Grid Mode: When the grid voltage is stable and there is no power failure, the UPS system operates in grid mode. The rectifier provides the regulated dc-link voltage to feed the inverter while the bidirectional converter keeps charging the battery bank.

Battery Mode: In case of power failure or voltage sag at input, the magnetic contactor (MC) is opened and the rectifier is disabled. Then power is supplied to the load by the battery which uses the battery discharger and the inverter. The value of the dc-link capacitor is kept high in order to provide sufficient energy to the inverter during the transition between the battery mode and grid mode of operation.

Bypass switch has been added in the system to increase the reliability of the system. In case of internal fault in the system or overloading and overheating of the circuit, the bypass switch turns ON and provides a direct path for the power from the utility grid to the connected load [2].

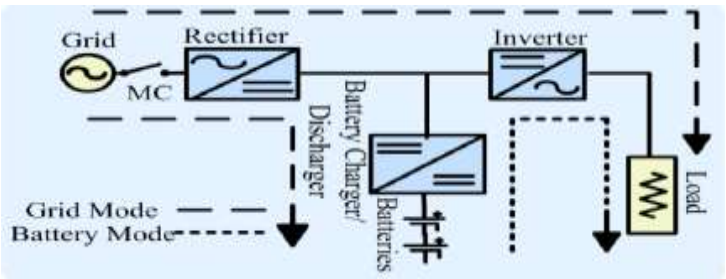

Figure. 2. Modes of operation of proposed UPS system [41]

B. Bidirectional converter

A new non-isolated bidirectional dc-dc converter with coupled inductor has been proposed which works as battery charger/discharger and operates between battery bank and the dc-link. The converter has following advantages.

1. High voltage gain in both the buck and boost mode.

2. Less number of passive components in the circuit.
3. Only three active switches are used to perform bidirectional operation.
4. Zero Voltage Switching (ZVS), synchronous rectification, and voltage clamping circuit are used that reduces the switching and conduction losses.

Coupled inductor has been used with LP as primary inductance and LS as the secondary inductance. The capacitor Cb2 inserted in the main power across the primary and secondary windings of the transformer gives high voltage conversion ratio and reduces the peak current stress allowing continuous current in the primary. Also, voltage stress of the capacitor Cb2 is minimum at this position in the circuit.

1. ***Battery Charging/Buck Operation***

The characteristic waveforms of the converter during battery charging mode are shown in Fig. 3. D1 is the duty cycle of S3 and Sax while D3 is the duty cycle of switch S4. Both D1 and D3 are related to each other by a relationship D1 (= 1− D3). Lm is the magnetizing inductance of the coupled inductor with turns ratio N = N2/N1, where N1 is the number of turns in primary winding and N2 is the number of turns for secondary winding. The operation of the circuit during battery charging mode in each interval is shown in Fig. 4.

Interval 1 (t0 ~ t1): The Switch S4 remains ON while the switches S3 & Sax are OFF during interval 1. The current *i*LS flows from dc-link to the battery bank through the capacitor Cb2 and both the windings of the coupled inductor. Applying KVL, we get (1).

Vd=VLS+VCb2+VLP+VBat (1)

Vd=VLP(1+N)+VCb2+VBat (2)

The diode Db3 is also conducting with continuous inductor current *i*Lb into the battery bank. Hence, VBat is the voltage across inductor Lb.

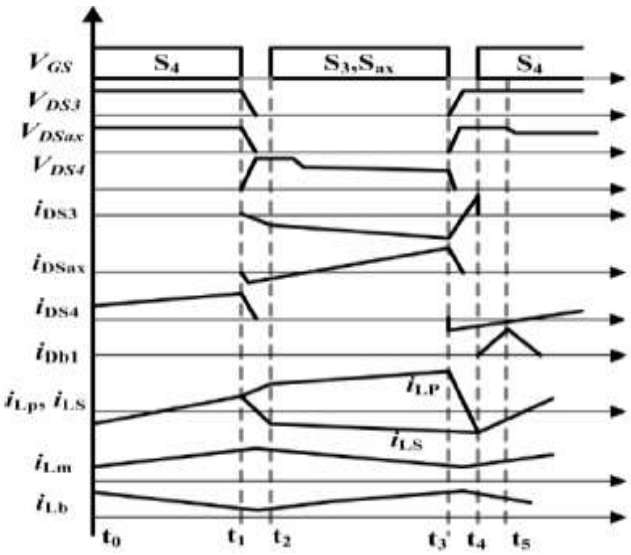

Figure. 3. Characteristic waveforms of the buck mode of operation

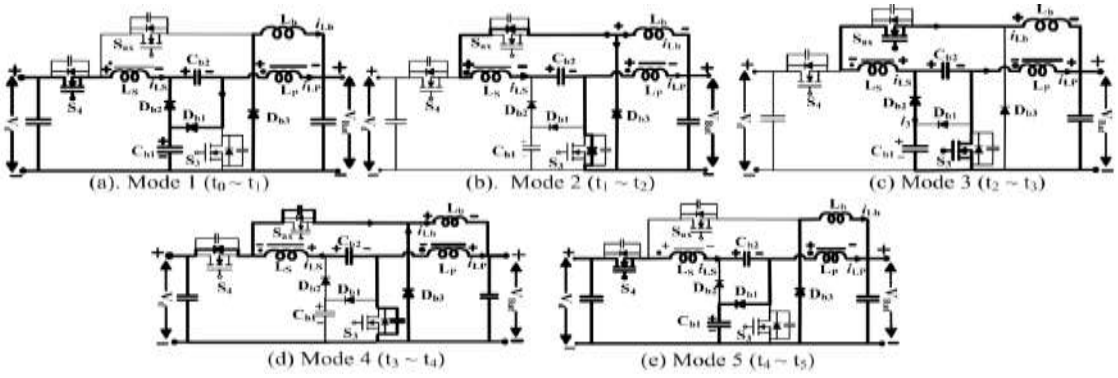

Figure. 4 Topological stages in buck mode: (a) Mode 1; (b) Mode 2; (c) Mode 3; (d) Mode 4; (e) Mode 5.

Interval 2 (t1 ~ t2): At the start, the switch S4 turns OFF. Due to the storage energy in the leakage inductor, the polarities are reversed across the primary and secondary windings (LS & LP) of the coupled inductor. Switch S4 is OFF in this mode, but the secondary current *i*LS is still conducting, so the switch Sax body diode is forward bias in order to keep the current *i*LS flowing. The diode Db3 remains forward biased in this mode. The body diode of switch S3 gets forward biased as the secondary current *i*LS decreases, however the primary current *i*LP remains the same.

Interval 3 (t2 ~ t3): Both the Switches S3 and Sax turns ON following zero voltage switching (ZVS) condition. The capacitor Cb2 starts discharging across battery bank through the switch Sax and inductor Lb. Thus, the secondary current is induced in reverse by discharging capacitor Cb2. Clamp capacitor Cb1 also discharges through the diode Db2 by adding small current *i*3 into the secondary current flowing into the battery bank.
Using the voltage second balance, VCb2 will be,
VCb2= V*Lb*+VBat+VLS (3)
The stored energy in the coupled inductor is released by primary current through the switch S3 into battery bank. Using the voltage-second balance, the VLb is given by,
D1VLb=D3VBat (4)
Primary winding voltage VLP can be obtained as, D3VLP=D1VBat (5)
Putting (4) and the values of VLb and VLP in (2), the voltage gain during buck mode of operation is given by equation,
Gbuck=VBatVd⁄=[D3(1−D3)][2N(1−D3)2+1]⁄ (6)

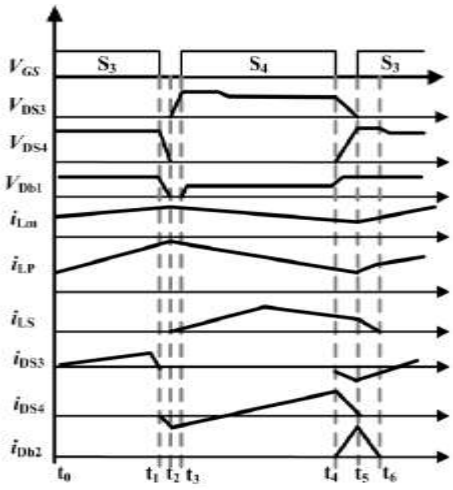

Figure. 5 Characteristic waveforms of the boost mode

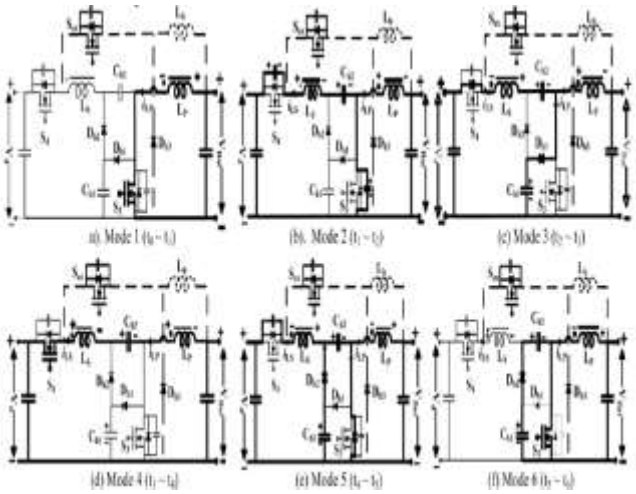

Figure. 6. Topological stages in boost mode: (a) Mode 1; (b) Mode 2; (c) Mode 3; (d) Mode 4; (e) Mode 5; (f) Mode

Interval 4 (t3 ~ t4): Both the switches S3 and Sax turn OFF at the start of this mode. The primary and secondary winding currents *i*LP & *i*LS will continue conduction due to the leakage inductance of the coupled inductor. The secondary current will charge the parasitic capacitance of the switches S3 & Sax, and discharge the parasitic capacitance of the switch S4. When the voltage across the switch Sax equals to Vd, the body diode of the switch S4 get forward biased. The primary current *i*LP starts decreasing unless it gets equal to the secondary current *i*LS, then this mode finishes.
Interval 5 (t4 ~ t5): The switch S4 turns ON under zero voltage switching (ZVS) condition. The capacitor Cb1 is charges through the clamped diode Db1. The primary and secondary current starts increasing. At the end of this mode, the circuit starts repeating interval 1of the next cycle.

1. ***Battery Discharging/Boost Operation***
The characteristic waveform of the bidirectional converter during battery discharge mode is shown in Fig. 5. The bidirectional converter steps up the low battery bank voltage to high dc-link voltage. The switch Sax remains OFF during battery discharging. The battery discharger operation during each interval is shown in Fig. 6.

Interval 1 (t0 ~ t1): During interval 1, the switch S3 was ON, while the switch S4 was OFF. Low battery bank voltage is applied at the low voltage side of the circuit. Capacitor Cb2 remains charged before interval 1 and the magnetizing current *i*Lm of the coupled inductor increases linearly as shown in the Fig. 5. Applying KVL, we get,

V_{Bat}=VLp=VLSN⁄(7)

The voltage across the primary winding may be derived using voltage second balance. VLPD3=VBatD1 (8)

Interval 2 (t1 ~ t2): The switch S3 turns OFF in interval 2. The primary current *i*LP charges the parasitic capacitance across the switch S3 and the secondary current *i*LS discharges the parasitic capacitance across switch S4. When the voltage across switch S3 becomes equal to the capacitor voltage VCb1, this interval finishes

Interval 3 (t2 ~ t3): Since the switch S3 is OFF, leakage inductance causes the primary current *i*LP to decrease while the secondary current *i*LS increases. As a result, the body diode of switch S4 gets forward biased. Capacitor Cb1 starts charging through diode Db1 because the voltage across the switch S3 gets higher than capacitor Cb1. This limits the voltage stress across the switch S3. The voltage across the C1 is given by,

VC1=V_{bat}+VLP (9)

Using (7),

VC1= VBatD3⁄(10)

Interval 4 (t3 ~ t4): the switch S4 turns ON under the condition of zero voltage switching (ZVS). The primary and secondary windings of the coupled inductor and the capacitor Cb2 are all now connected in series to transfer the energy to the dc-link. The *i*LS starts increasing until it reaches the *i*LP, then it follows the *i*LP till the end of the interval 4. Thus, the energy stored in the primary and secondary windings discharges across the dc-link. Both the diodes Db1 and Db2 remain reverse biased during this interval as shown in Fig. 6(d). Using voltage second balance, we get (11)

Vd=V_{Bat}+VLS+VC2+VLp (11)

Vd=VBat+VC2+(N+1)VLP (12)

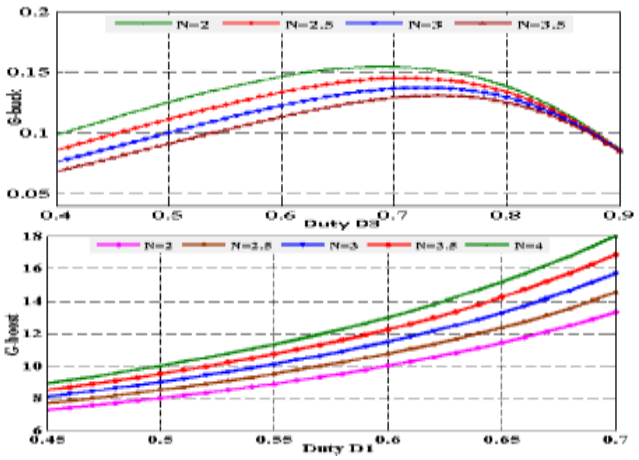

Figure. 7. Voltage conversion ratio w.r.t duty cycle D1 and D3.

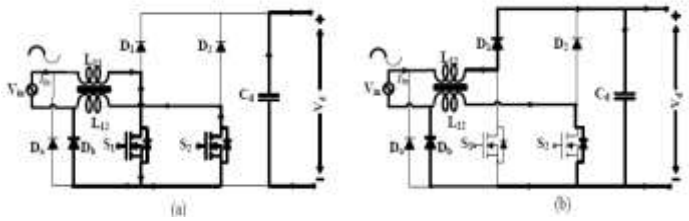

Figure. 8. Rectifier operation during positive half cycle; a) Switches S1 & S2 are ON. b) Switches S1 & S2 are OFF

Interval 5 (t4 ~ t5): During this interval, the switch S4 turns OFF. The current *i*LS charges the parasitic capacitance of the switch S4. The capacitor Cb1 starts discharging across the capacitor Cb2, through the diode Db2.

VCb2=VCb1=V_{Bat}D3⁄(13)

By putting (8) and (13) in (12), Voltage gain of the circuit is.

Vd=V_{Bat}+V_{Bat}D3+(N+1)D1D3⁄VBat⁄(14)

Gboost=VdVBat=⁄(2+ND1)(1−D1)⁄(15)

The body diode of the switch S3 starts forward biased because of the polarities of the capacitor Cb2 and inductor LP.

Interval 6 (t5 ~ t6): During interval 6, the switch S3 turns ON under the condition of zero voltage switching. Since S3 is not deriving any current from the clamped circuit, thus the switching losses remain low due to ZVS and the efficiency of the circuit increases. When both the VCb1 and VCb2 get equal, then the next switching cycle starts and repeats the operation in interval 1.

The turn ratio N is selected as such to satisfy the Gboost and Gbuck gains for required DC-link and battery bank voltage. Fig. 7 shows the voltage gain of buck and boost modes with respect to duty cycle D3 and D1 respectively at different turn ratio. Turn ratio N = 4 satisfies the operation of bidirectional converter between the required dc-link and battery bank

The voltage conversion ratio of the proposed converter shows more diversity as compared to, with less number of switches. In [10] the authors have shown high gain ratio but with five switches, that increases the size and cost of the circuit. The size of the proposed circuit is considerably small with small heat sink for the given power rating, and only few passive auxiliary components are used. Since the battery voltage is very low and high current flows from the battery bank into the converter. Thus, it increases conduction losses. However, the switching losses are not significant as all the switches of the bidirectional DC-DC converter are following ZVS condition. The high current can increase the size and cost of the system, hence limits the operation of proposed topology for very high power applications where the input current can be very high.

C. Rectifier

The rectifier performing the unity power factor consists of bridgeless PFC boost rectifier. The bridgeless PFC boost rectifier does not use the full wave bridge rectifier, reducing one semiconductor device in the main current path. Thus, the conduction losses are reduced, which increases the efficiency of the rectifier. The bridgeless PFC has the advantage of reducing the conduction loss by 30% [11]. This topology is suitable for applications where high power density and high efficiency are required. The bridgeless rectifier consists of two boost converters, each operating in the half cycle of the AC supply. By adding two slow diodes Da ~ Db, the common mode noise (EMI Losses) can be suppressed considerably and high efficiency can be achieved as compared to conventional rectifier. Both the switches S1 and S2 of the rectifier are driven by the same gate signal, thus makes the control of the circuit quite easy. The inductors L11 and L12 of the boost rectifier can be wound in the same core in order to increase the utilization of magnetic material [12].

The operation of the rectifier during only positive half cycle has been shown in Fig. 8. The switch S1 turns ON, as the input voltage Vin (AC) turns positive. The current flows from the input through the inductor L11 and L12, storing the energy in both the inductors. The change in the input current *iin* is same as the change in the inductor current, given by (16).

$\Delta iin = 1\ L11{+}L12\ VinDTs$ (16)

When the switch S1 turns OFF, the energy is released by the inductors. The current flows through the diode D1 into the dc-link Vd, returning through the body diode of the switch S2 into

the input supply. The input current in D1 and S2 is same as the inductor current given by (13),

$\Delta iin = 1\ L11{+}L12\ (Vin - V\ )(1 - D)Ts$ (17)

Depending on the duty cycle D of both the switches S1 and S2, the input current variation for one complete switching cycle TS is given by,

$(L11 + L12)\ \Delta iin\ TS = VinDTs + (Vin - V\ )(1 - D)Ts$ (18)

EMI noise is generated due to high-frequency switching that is leaked through the parasitic capacitance from the converter to the ground. Therefore, the EMI noise suppression diode Da

and Db are used, as they provide the conducting path between the output bus and the input line during both the positive and negative cycles, thus the voltage potential of the output bus is stabilized [14].

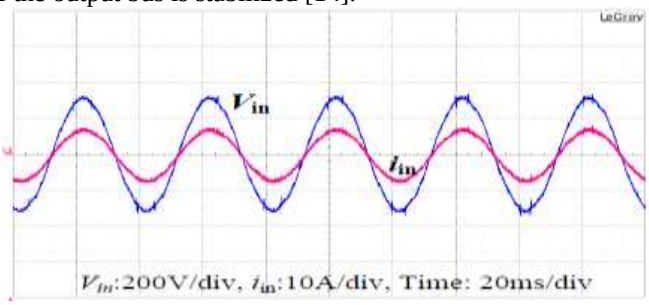

Figure. 9: Input voltage and current waveform.

III. EXPERIMENTAL RESULTS

To verify the performance of the proposed UPS system, a laboratory prototype has been implemented with the specifications shown in Table 2. The control scheme for inverter, rectifier, and battery charger/discharger has been implemented using DSP TMS320F28335. The design parameters of the rectifier, battery charger/discharger, and inverter are shown in Table 3, Table 4, and Table 5 respectively. The backup storage system consists of two batteries (each battery is 24V/35 Ah), or parallel batteries depending upon the backup time for the connected load.

The efficiency is maximum 93% during battery mode and 90% during grid mode of operation shown in Table 6. Thus utilizing soft switching in bi-directional converter reduces the switching losses and increases the efficiency of the system. The efficiency in battery mode is high as compare to grid mode, because less number of power stages is operation during this mode. The efficiency is slightly less for transformerless system, due to high battery charging current. The proposed UPS shows the distinct improvement in terms of reducing the size of the battery bank, decreasing the overall volume and weight of the system.

TABLE 2
SPECIFICATIONS OF THE PROPOSED UPS SYSTEM

Parameters	Symbol	Value
Input Voltage	V_{in}	230V
Output Voltage	V_{out}	230V
Grid Frequency	f_r	50Hz
No. of Batteries	V_b	2 parallel connected (24V/35Ah)
Max. Output Power	$P_{o,max}$	1kVA
DC Link Voltage	V_d	360V

TABLE 3
DESIGN PARAMETERS OF THE RECTIFIER

Parameters	Symbol	Value
Input Inductor	L_{11}, L_{12}	100µH
Diodes	D_1, D_2	--
Switches	S_1, S_2	MOSFET
Slow Diodes	D_a, D_b	--
Switching Frequency	f_s	30kHz

TABLE 4
SPECIFICATION OF BATTERY CHARGER/DISCHARGER

Parameter	Symbol	Value
DC Link Voltage	V_d	360V
Battery Bank Voltage	V_b	24V
Switching Frequency	f_s	30kHz
Coupled Inductor	L_P, L_S	L_m=107µH; Turns ratio=4
Inductor	L_b	300µH
Capacitor	C_{b1}, C_{b2}, C_d	2x2.2µF, 1900µH
Switches	S_3, S_4, S_{ax}	MOSFET
Diodes	D_{b1}, D_{b2}, D_3	Fast recovery diode

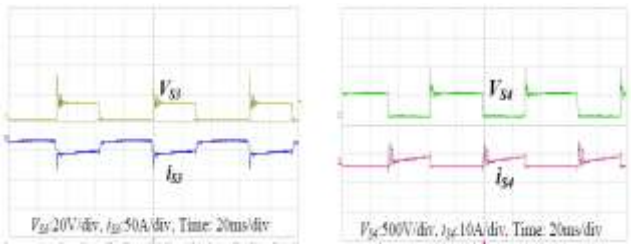

Figure.10 Drain to source voltage and current of switches S3 and S4 during battery charging (buck Mode)

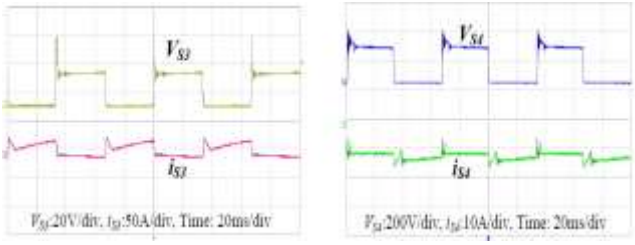

Figure. 11 Drain to source voltage and current of switches S3 and S4 during battery discharging (Boost Mode)

TABLE 5
DESIGN PARAMETERS OF THE INVERTER

Parameter	Symbol	Value
Switching Frequency	f_s	20kHz
Switches	$S_3 \sim S_4$	MOSFET
Output Filter Inductor	L_f	570mH
Output Filter Capacitor	C_f	6.6μH
Switching Frequency	f_{cut}	1.7kHz

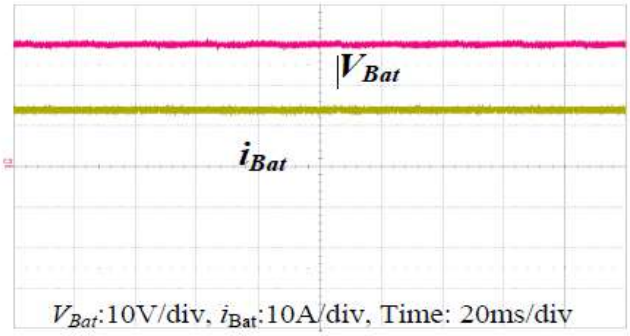

Figure.12. Voltage and current of battery charger

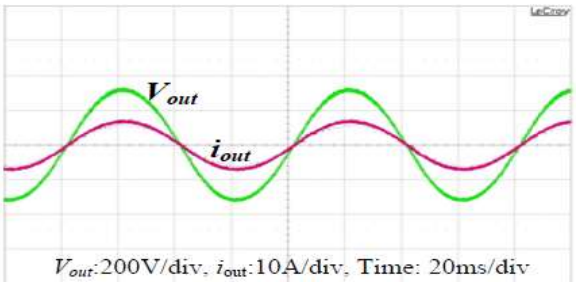

Figure.13 Output voltage and current for linear load

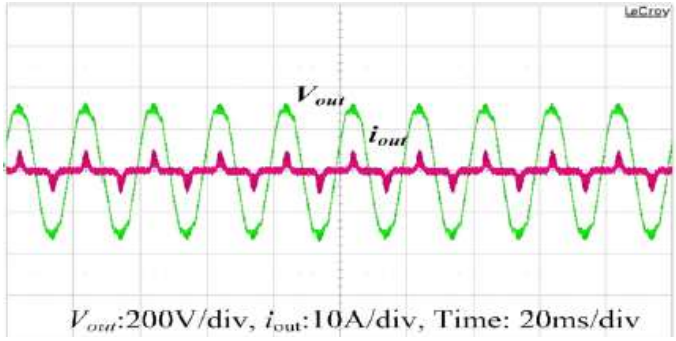

Figure.14 Output voltage and current for non-linear load

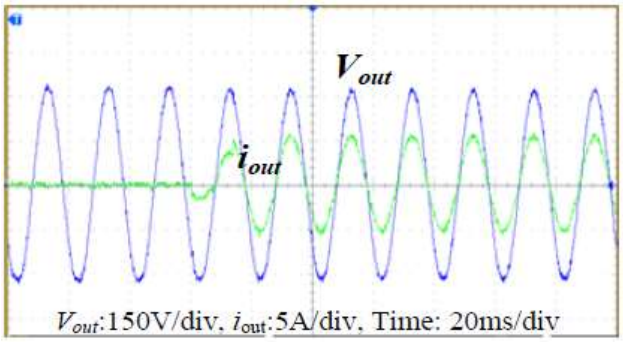

Figure. 15 Experimental waveform of step change, 0 to 100%

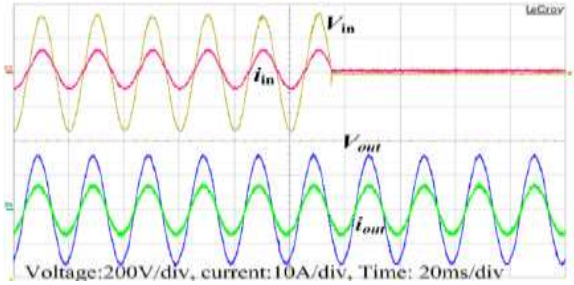

Figure. 16 Transition from grid to battery mode, Input voltage *Vin* and current *Iin*, Output voltag e *Vout* and current *Iout*

The utility input voltage and current waveform in grid mode of operation is shown in the Fig. 9. The input current waveform is very close to the sinusoidal and has almost unity power factor with THD 4.5%. Fig. 10 and 11 shows drain to source voltage of the switches S3 and S4 of the bidirectional converter (battery charger) during both the buck and boost mode of operation respectively. Both the switches are operating under the condition of zero voltage switching (ZVS). Similarly the output voltage and current of the bidirectional converter during battery charging has been shown in Fig. 12. The output voltage and current waveform during linear load is shown in Fig. 13. The waveform is sinusoidal with THD less than 1%. Also the system is connected with the non-linear load designed according to the standard of IEC62040-3. The system shows good performance with THD of 1.25% for the non-linear load as shown in the Fig. 14.

The Fig. 15 show the output voltage and current waveform during step change in load from 0 to 100% and form 100% to 0. The system shows good response to step changes and provide regulated output voltage regardless of theload changes. When the grid power is interrupted and the system switches from grid mode to battery mode. The rectifier is no more in operation and the battery charger/discharger operates in discharging mode giving regulated dc-link voltage. The transient effect in the output voltage is very small and the UPS system provides uninterruptible power to the load as shown in Fig. 16. Similarly the transition from battery mode back to grid mode upon the restoration of the grid power is shown in Fig. 17. Simple RC snubber has been used to discharge the inductors L11 and L12, preventing the overvoltage spike when the MC opens.

Fig. 18 shows the efficiency graph with maximum efficiency of 94% during battery mode and 92% during grid mode of operation. Thus utilizing soft switching in bidirectioanl converter reduces the switch losses and increases the efficiency of the system. The efficiency in battery mode is high as compare to grid mode, because less number of power stages are operation during this mode. The efficiency is slightly less for transformerless system, due to high battery charging current. Table 6 shows the comparison of the different transformerless UPS system. The proposed UPS shows the distinct improvement in terms of reducing the size of the battery bank, decreasing the overall volume and weight of the system.

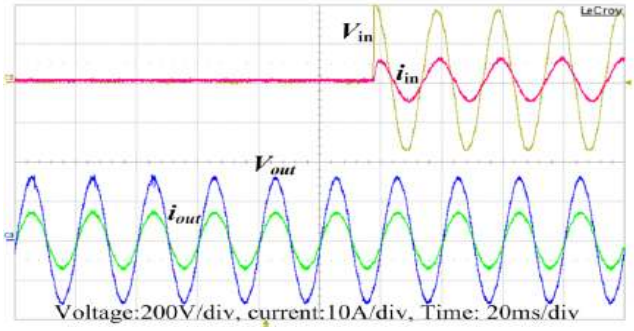

Figure. 17. Transition from battery to grid mode, Input voltage *Vin* and current *Iin*, Output voltage *Vout* and current *Iout*

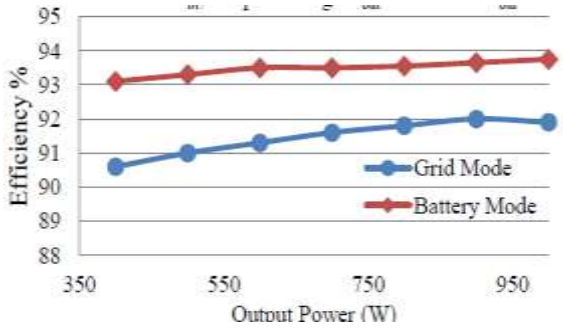

Figure. 18 Efficiency graph in grid and battery mode

IV. CONCLUSION

A single phase transformerless online uninterruptible power supply has been proposed in this paper. A bridgeless boost rectifier has been used with average current control method that increases the efficiency of the system and provides the power factor correction. A new bidirectional converter for battery charging/discharging has been implemented which ensures transformerless operation and reduces the battery bank significantly. A new control for the inverter provides regulated sinusoidal output voltage with low THD for both linear and non-linear load. Overall the volume of the system is minimized by reducing the size, weight, and battery bank of the system. The experimental results show good dynamic and steady state performance. It may be recommended to extend this proposed UPS system to three phase transformerless online UPS system.

REFERENCES

[1] A. Lahyani, P. Venet, A. Guermazi, and A. Troudi, "Battery/supercapacitors combination in uninterruptible power supply (UPS)," IEEE Transactions on Power Electronics, vol. 28, pp. 1509- 1522, 2013.

[2] Y. Zhang, M. Yu, F. Liu, and Y. Kang, "Instantaneous current-sharing control strategy for parallel operation of UPS modules using virtual impedance," IEEE Transactions on Power Electronics, vol. 28, pp. 432- 440, 2013.

[3] B. Zhao, Q. Song, W. Liu, and Y. Xiao, "Next-generation multifunctional modular intelligent UPS system for smart grid," IEEE Transactions on Industrial Electronics, vol. 60, pp. 3602-3618, 2013.

[4] C. G. Branco, R. P. Torrico-Bascope, C. M. Cruz, and F. de A Lima, "Proposal of three-phase high-frequency transformer isolation UPS topologies for distributed generation applications," IEEE Transactions on Industrial Electronics, vol. 60, pp. 1520-1531, 2013.

[5] S. Karve, "Three of a kind [UPS topologies, IEC standard]," IEE Review, vol. 46, pp. 27-31, 2000.

[6] F. Botterón and H. Pinheiro, "A three-phase UPS that complies with the standard IEC 62040-3," IEEE Transactions on Industrial Electronics, vol. 54, pp. 2120-2136, 2007.

[7] E.-H. Kim, J.-M. Kwon, and B.-H. Kwon, "Transformerless three-phase on-line UPS with high performance," IET Power Electronics, vol. 2, pp.103-112, 2009.

[8] M. R. Reinert, C. Rech, M. Mezaroba, and L. Michels, "Transformerless double-conversion UPS using a regenerative snubber circuit," in Power Electronics Conference, COBEP'09. Brazilian, 2009, pp. 564-570.

[9] S. B. Lim, H.-J. Lee, J.-P. Lee, Y.-H. Lee and S.-C. Hong, "A New single phase double-conversion UPS using PWAM method," in IEEE6th International Conference on Power Electronics and Motion Control,IPEMC'09, pp. 2507-2511, 2009.

[10] Y. Zhan, Y. Guo, J. Zhu, and H. Wang, "Intelligent uninterruptible power supply system with back-up fuel cell/battery hybrid power source," Journal of Power Sources, vol. 179, pp. 745-753, 2008.

[11] B. Su and Z. Lu, "An interleaved totem-pole boost bridgeless rectifier with reduced reverse-recovery problems for power factor correction," IEEE Transactions on Power Electronics, vol. 25, pp. 1406-1415, 2010.

[12] Y. Jang and M. M. Jovanovic, "A bridgeless PFC boost rectifier with optimized magnetic utilization," IEEE Transactions on Power Electronics, vol. 24, pp. 85-93, 2009.

[13] P. Kong, S. Wang, and F. C. Lee, "Common mode EMI noise suppression for bridgeless PFC converters," IEEE Transactions on Power Electronics, vol. 23, pp. 291-297, 2008.

[14] Muhammad Aamir, and Saad Mekhilef, Senior Member, IEEE, "Online Transformerless Uninterruptible Power Supply (UPS) System with a Smaller Battery Bank for Low Power Applications," IEEE Transactions on Power Electronics, DOI 10.1109/TPEL.2016.2537834.